APPLYING SPECTROSCOPIC ANALYSIS METHODS TO STUDY THE PHYSICAL PROPERTIES OF MOS_2 AND ITS ADSORPTION ISOTHERM AND THERMODYNAMIC OF TARTRAZINE

Đến tòa soạn 01-03-2021

Mac Van Hung, Vu Anh Tuan
School of Chemical Engineering, Hanoi University of Science and Technology, Hanoi, Vietnam

TÓM TẮT

ỨNG DỤNG CÁC PHƯƠNG PHÁP PHÂN TÍCH QUANG PHỔ ĐỂ NGHIÊN CỨU CÁC TÍNH CHẤT VẬT LÝ CỦA MOS_2 VÀ ĐẲNG NHIỆT HẤP PHỤ VÀ NHIỆT ĐỘNG HỌC CỦA TARTRAZINE

Trong nghiên cứu này, MoS_2 được tổng hợp bằng phương pháp thủy nhiệt để hấp phụ tartrazine trong môi trường nước. Các phương pháp phân tích quang phổ được áp dụng để khảo sát các tính chất vật lý của mẫu tổng hợp và đường đẳng nhiệt hấp phụ và nhiệt động học của nó. Tinh thể của MoS_2 có cấu trúc lục giác, hình thái của MoS_2 là hình dạng giống san hô được kết hợp từ nhiều tấm nano có độ dày khoảng 10 nm. Đường đẳng nhiệt hấp phụ được thực hiện bằng cách sử dụng các mô hình Langmuir và Freundlich. Kết quả cho thấy dữ liệu thực nghiệm được mô tả bởi mô hình Langmuir phù hợp hơn so với mô hình Freundlich. Dung lượng hấp phụ đơn lớp tối đa, hằng số Langmuir và R^2 lần lượt là 26,7 mg/g, 0,78 L/g và 0,984. Các thông số nhiệt động học, $\Delta G°$, $\Delta H°$ và $\Delta S°$ đã được tính toán xác nhận quá trình hấp phụ là nhiệt động học toả nhiệt và tự phát.

Từ khoá: *Phân tích, quang phổ, MoS_2, đẳng nhiệt hấp phụ, nhiệt động lực học.*

1. INTRODUCTION

Molybdenum disulfide (MoS_2) belongs to layered transition metal dichalcogenides (TMD). It is a layered material with molybdenum sandwiched between two sulfide layers by covalent forces, forming S–Mo–S layer and the weak Van der Waals forces, jointing S – Mo – S layers. In appearance and feel, molybdenum disulfide is like graphite. Bulk MoS_2 is a diamagnetic, indirect bandgap semiconductor similar to silicon, with a bandgap of 1.23 eV [1]. Many papers have shown that MoS_2 could be applied in various sectors such as solid material lubricants [2], hydrogen evolution reaction [3], lithium batteries[4], and energy storage & conversion [5].

Recently, organic dyes usually use in various fields such as textile dyeing, cosmetic, paper making, and pesticide industries. It possesses a potential health hazard to all forms of life even at a very low concentration. Therefore, various methods have been applied to remove organic dyes from wastewater which include precipitation, adsorption, ion exchange, chemical oxidation, biological degradation, and coagulation [6]. In which, adsorption is believed to be a low-cost and rapid method for effective removal of organic dyes and has been widely used in water treatment.

Tartrazine is a synthetic lemon-yellow azo dye. It is considered as a typical organic contaminant and widely applied in many industries like foodstuff, medicine, cosmetics,

and textiles. Tartrazine is confirmed to highly toxic for humans due to causes of asthma, eczema, thyroid cancer [7].

In order to that, we fabricated MoS_2 by utilizing a hydrothermal method for adsorption of tartrazine. As-prepared sample was characterized by spectroscopic analysis methods (XRD, BET, FT-IR and SEM). The adsorption isotherm and thermodynamic of tartrazine on MoS_2 were investigated. In addition, the adsorption performance of MoS_2 was compared to other MoS_2 samples in literatures.

2. EXPERIMENTAL

2.1. Materials

Thioacetamide (C_2H_5NS, 99%) and sodium molybdate dihydrate ($Na_2MoO_4.2H_2O$, 99%) were purchased from China. Tartrazine (99%) was purchased from Sigma-Aldrich. All the chemicals were used without any purification and distilled water was used throughout the experiments.

2.2. Synthesis of MoS_2

MoS_2 was synthesized by the hydrothermal method using sodium molybdenum dihydrate and thioacetamide as the starting material. In a typical experiment, $Na_2MoO_4.2H_2O$ (0.54 g) and C_2H_5NS (0.36 g) were dissolved in 40 mL of distilled water and stirred for 60 min to form a transparent solution. The mixed solution was transferred into a Teflon-lined 100 mL stainless steel autoclave and heated at 200 °C for 48 h. Then, the autoclave was cooled to room temperature, the MoS_2 powder was collected by a vacuum filter, washed with distilled water and ethanol, and dried in an oven at 70 °C for 12 h.

2.3. Characterization

The crystalline phase of as-prepared MoS_2 was investigated by X-ray power diffraction. XRD pattern was obtained by using XRD-diffractometer (Bruker D8 Advance, Germany) with CuKα irradiation (40 kV, 40 mA). Fourier modified infrared (FT-IR) spectra were recorded on the JASCO FT/IR-4600 spectrum analyzer. Scanning electron microscopy (SEM) image of MoS_2 material was recorded using an FE-SEM, JEOL-7600F, working at 15 kV. Textural properties were measured via N_2 adsorption/desorption isotherm using a micromeritics (Gemini VII). The specific surface area was calculated by using the Brunauer-Emmett-Teller (BET) method and the pore size distribution was obtained by using the Barrett-Joyner-Halenda (BJH) method.

2.3. Adsorption experiment

The adsorption experiments were performed by batch reactor, a certain amount of MoS_2 (0.08g) was poured into a beaker containing 100 mL of tartrazine under magnetic stirring. After a certain time, about 2 mL of suspension was withdrawn from the beaker and then filtered to remove the adsorbent. The concentration of dye was analyzed by a UV-vis spectrophotometer (Agilent 8453). The equilibrium adsorption capacity (q_e) and the removal efficiency (Re) of the dye are determined by equations (1) and (2), respectively.

$$q_e = \frac{(C_o - C_e) \times V}{m} \quad (1)$$

$$Re = \frac{C_o - C_t}{C_o} \times 100\% \quad (2)$$

where q_e (mg/g) is the equilibrium adsorption amount, C_o (mg/L), C_e (mg/L), and C_t (mg/L) are the initial, equilibrium, and concentration at t time, respectively; V (L) is the volume of dye solution; and m (g) is the mass of MoS_2.

3. RESULT AND DISCUSSION

3.1. Characterization of material

The XRD pattern of the MoS_2 sample was presented in Figure 1 (a). The diffraction peaks at 2θ values of 33.28°, 39.58°, and 58.76° could be assigned to (100), (103), and (110) planes, which reflected hexagonal structure of MoS_2 [8].

The FT-IR spectrum is shown in Figure 1 (b). It could be observed the strong band at 3586 cm^{-1}, it corresponded to the fluctuation of the O-H bond in the adsorbing water (H-O-H) on the surface of MoS_2. The strong region at 1638 cm^{-1} was assigned to the C = O covalent oscillating bond of the carboxyl group (–COOH). The main bands at 1128 cm^{-1} and 658 cm^{-1} could be assigned to the oscillation of the S = O bond in MoS_2, the characteristic of the bending oscillation of S_xO_y, respectively [9,10].

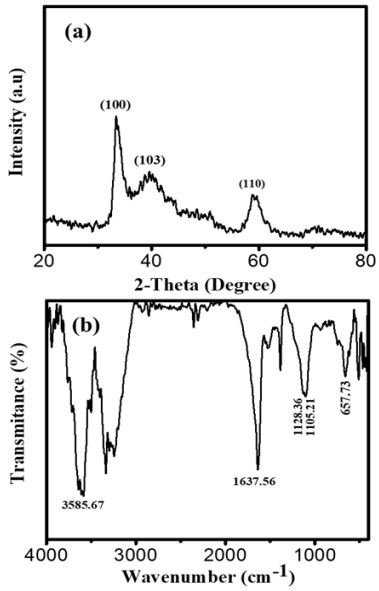

Figure 1. (a) XRD pattern and (b) FT – IR spectra of MoS_2.

The SEM result of MoS_2 is presented in Figure 2. The as-prepared MoS_2 has a coral-like structure, the agglomerated shape was 80-100 nm in size, which was consisted of many nano-sheets with a thickness of about 10 nm. It resulted in the larger pore in the sample and the relatively high surface area (in Table 1). These could be significant factor for accelerating the adsorption capacity and adsorption rate of dyes on MoS_2.

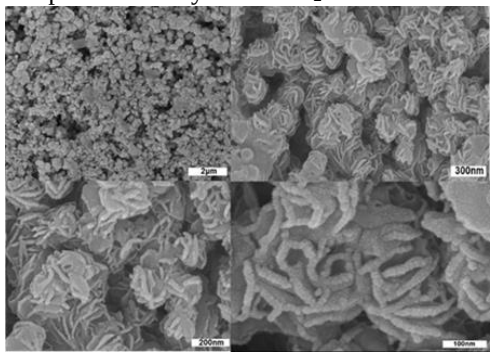

Figure 2. SEM images of MoS_2

The N_2 adsorption/desorption isotherm and Barrett–Joyner–Halenda (BJH) pore size distribution plot of MoS_2 are shown in Figure 3. The isotherm was identified as classical type IV according to the IUPAC classification [11], which was characteristic of the mesoporous structure. Table 1 summarizes the physical parameters of the MoS_2 sample. The BET surface area, pore volume, and pore diameter of MoS_2 were 83.9 m^2/g, 0.48 cm^3, and 18.9 nm, respectively.

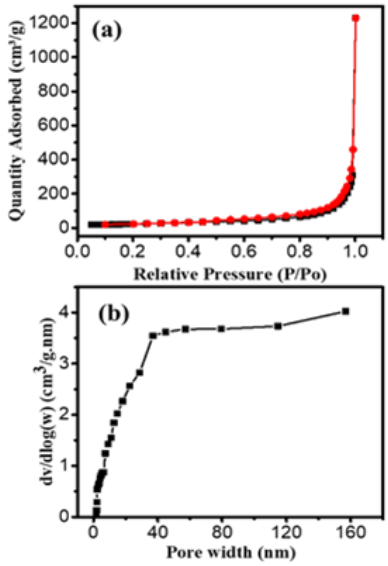

Figure 3. (a) N_2 adsorption/desorption isotherm and (b) pore size distribution of MoS_2.

Table 1. Physical parameters of the MoS_2 material.

Sample	S_{BET} (m^2/g)	Pore volume (cm^3/g)	Average pore diameter (nm)
MoS_2	83.9	0.48	18.9

3.3. Adsorption isotherms

The adsorption isotherm shows how the adsorbed molecules distribute between the liquid phase and solid phase when the adsorption equilibrium has been established.

The adsorption isotherms studies were carried out using Langmuir and Freundlich models. The Langmuir model (Eq.3) assumes that adsorption occurs on a homogeneous surface by monolayer coverage and no subsequent interaction between adsorbed species. The Freundlich model (Eq.4) is an empirical model based on multiplayer adsorption on heterogeneous surfaces.

$$\frac{1}{q_e} = \frac{1}{q_{max}} + \frac{1}{C_e . k_L . q_{max}} \quad (3)$$

$$\ln q_e = \ln k_F + \frac{1}{n} \ln C_e \quad (4)$$

where C_e (mg/L) is the equilibrium concentration, q_e (mg/g) is the equilibrium adsorption capacity, q_{max} (mg/g) represents the maximum adsorption capacity, k_L and k_F is the Langmuir and Freundlich adsorption constant, respectively, and n is the Freundlich exponential coefficient.

The Langmuir and Freundlich isotherm models which were fitted experimental data were presented in Figure 4. The parameters for tartrazine adsorption on MoS_2 calculated from the two models are shown in Table 2.

Table 2. Adsorption isotherm parameters.

Isotherm model	Parameter	Value
Langmuir	q_{max} (mg/g)	26.7
	k_L (L/mg)	0.78
	R^2	0.984
Freundlich	k_F (mg/g)	17.5
	n	8.7
	R^2	0.975

The results from Table 2 show that the R^2 value of the Langmuir isotherm (R^2 = 0.984) was higher than that of the Freundlich isotherm (R^2 = 0.975). It can be concluded that the Langmuir model was more suitable than Freundlich model to describe the adsorption of tartrazine on MoS_2. It indicated that the interaction between the tartrazine molecules and the MoS_2 surface was homogeneous and monolayer adsorption behavior.

Table 3 shows the comparison of the morphology, surface area, maximum monolayer adsorption capacity of as-prepared MoS_2 sample, and MoS_2 samples synthesized through the hydrothermal method. It could be observed that the specific surface area of MoS_2 in this study is quite high (83.9 m^2/g) which was only lower than fungus-like nanosheet MoS_2. However, its maximum monolayer adsorption capacity of as-prepared MoS_2 (26.7 mg/g) was lower than those of other materials (39.03 - 425.50 mg/g). This can be assigned to reasons following: (1) after dispersing into the water the surface of the negatively charged MoS_2 particles increases the electrostatic repulsion between it and the anionic dye (tartrazine), making the adsorption capacity decrease [12,13]; (2) the structure and charge of each dye resulting in the difference of adsorption capacity on MoS_2.

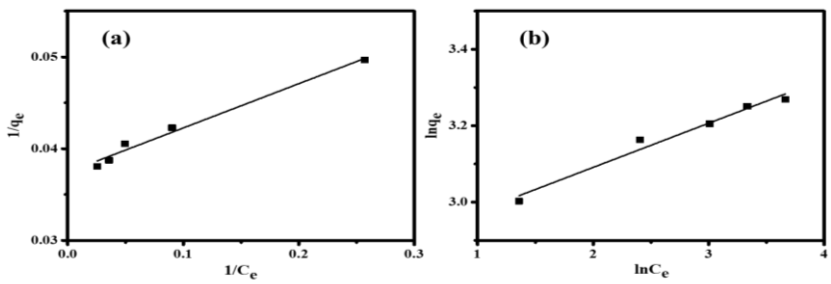

Figure 4. Langmuir (a) and Freundlich models (b) for tartrazine adsorption on MoS_2.

Table 3. Comparison of the properties of MoS_2 with various adsorbents.

No.	Material	Morphology	BET surface area (m^2/g)	Dye	Maximum monolayer adsorption capacity (mg/g)	Reference
1	MoS_2	nano-sheet	67.8	Bisphenol A	39.03	[14]
2	MoS_2	fungus-like nanosheet	107.0	Congo red	285.7	[15]
3	MoS_2	multi-layered nanosheets	62,5	Methylene blue, Methyl orange	_	[16]
4	MoO_3/MoS_2	nanorod shape	43,5	Rhodamine B	425,5	[17]
5	MoS_2	3D flower-like structure	63.9	Rhodamine B Methylene blue	291 208	[12]
6	MoS_2	Hierarchical microspheres nanosheets	_	Methylene blue	87,4	[18]
7	MoS_2	coral-like structure	83.9	Tartrazine	26.7	In this work

3.2. Adsorption thermodynamics

The thermodynamic parameters were very important to understand the kinetics of adsorption, which were included free energy (ΔG°), enthalpy (ΔH°), and entropy (ΔS°), were calculated by using the following equations (5), (6), and (7).

$$\Delta G^{\circ} = -RT\ln k_c \quad (5)$$

$$k_c = \frac{q_e}{C_e} \quad (6)$$

$$\ln k_c = -\frac{\Delta H^{\circ}}{RT} + \frac{\Delta S^{\circ}}{R} \quad (7)$$

where k_c is the equilibrium constant, (q_e/C_e) is the distribution coefficient, T is the temperature in Kelvin and R is the universal gas constant (8.314 J/mol K).

The effect of temperature on adsorption capacity and Van't hoff plot for adsorption of tartrazine on MoS_2 are shown in Figure 5. The thermodynamic parameters were calculated from equations 5 and 7 at three different temperatures and the result was shown in Table 4. We can observe that the value ΔG° negative at all temperatures and it increased from -2.75 to -0.14 kJ/mol when the temperature increased from 293 to 313 °K, respectively, which indicates that the adsorption of tartrazine on MoS_2 was a spontaneous process. The value of ΔG° became more positive with the increase in temperature, suggested that higher temperature was less favorable for the adsorption of tartrazine on MoS_2. The negative value ΔH° (-41.02 kJ/mol) confirmed the exothermic nature of adsorption, which was also supported by the decline in the tartrazine adsorption removal ratios when the increased temperature. The negative value of ΔS° (-0.13 kJ/K/mol) reflected that there was a decrease in the degree of freedom of the adsorbed species [19].

Table 4. Thermodynamic parameters.

Temperature (K)	ΔG° (kJ.mol^{-1})	ΔH° (kJ.mol^{-1})	ΔS° (kJ.K^{-1}.mol^{-1})
293	-2.75	-41.02	-0.13
303	-1.32		
313	-0.14		

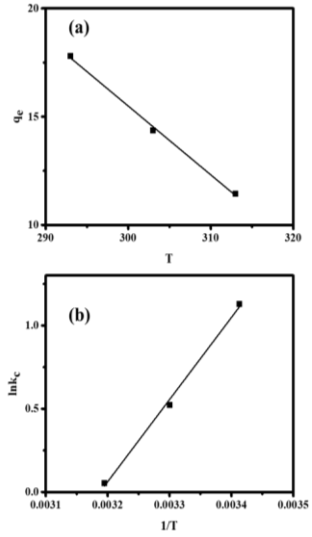

Figure 5. Effect of temperature on adsorption capacity (a), Van't hoff plot for adsorption of tartrazine on MoS_2 (b), respectively.

4. CONCLUSION

In summary, the coral-like MoS_2 has been successfully synthesized by a hydrothermal method. The spectroscopic analysis methods were applied to investigate the physical properties of as-prepared sample and its adsorption isotherm and the thermodynamic. MoS_2 had hexagonal structure and a relatively large specific surface area (83.9 m^2/g) compared to that in recent reports. The Langmuir model was more suitable than Freundlich model to describe the adsorption of tartrazine on MoS_2. The maximum monolayer adsorption capacity was 26.7 mg/g. The adsorption process is exothermic and spontaneous, as demonstrated by thermodynamic parameters.

REFERENCE

[1] U. Krishnan, M. Kaur, K. Singh, M. Kumar, A. Kumar, A synoptic review of MoS_2: Synthesis to applications, Superlattices and Microstructures 128 (2019) 274-297.

[2] H. Wu, L. Qin, G. Dong, M. Hua, S. Yang, J. Zhang, An investigation on the lubrication mechanism of MoS_2 nano sheet in point contact: The manner of particle entering the contact area, Tribology International 107 (2017) 48-55.

[3] D. Voiry, M. Salehi, R. Silva, T. Fujita, M.

Chen, T. Asefa, V.B. Shenoy, G. Eda, M. Chhowalla, Conducting MoS_2 nanosheets as catalysts for hydrogen evolution reaction, Nano letters 13 (2013) 6222-6227.
[4] C. Feng, J. Ma, H. Li, R. Zeng, Z. Guo, H. Liu, Synthesis of molybdenum disulfide (MoS_2) for lithium ion battery applications, Materials Research Bulletin 44 (2009) 1811-1815.
[5] Q. Yun, Q. Lu, X. Zhang, C. Tan, H. Zhang, Three-dimensional architectures constructed from transition-metal dichalcogenide nanomaterials for electrochemical energy storage and conversion, Angewandte Chemie International Edition 57 (2018) 626-646.
[6] G. Moussavi, M. Mahmoudi, Removal of azo and anthraquinone reactive dyes from industrial wastewaters using MgO nanoparticles, Journal of hazardous materials 168 (2009) 806-812.
[7] V.A. Tu, V.A. Tuan, A facile and fast solution chemistry synthesis of porous ZnO nanoparticles for high efficiency photodegradation of tartrazine, Vietnam Journal of Chemistry 56 (2018) 214-219.
[8] Y.-J. Yuan, J.-R. Tu, Z.-J. Ye, H.-W. Lu, Z.-G. Ji, B. Hu, Y.-H. Li, D.-P. Cao, Z.-T. Yu, Z.-G. Zou, Visible-light-driven hydrogen production from water in a noble-metal-free system catalyzed by zinc porphyrin sensitized MoS_2/ZnO, Dyes and Pigments 123 (2015) 285-292.
[9] J.H. Park, G. Choppala, S.J. Lee, N. Bolan, J.W. Chung, M. Edraki, Comparative sorption of Pb and Cd by biochars and its implication for metal immobilization in soils, Water, Air, & Soil Pollution 224 (2013) 1711.
[10] F. Maugé, J. Lamotte, N. Nesterenko, O. Manoilova, A. Tsyganenko, FT-IR study of surface properties of unsupported MoS_2, Catalysis today 70 (2001) 271-284.
[11] J. Rouquerol, F. Rouquerol, P. Llewellyn, G. Maurin, K.S. Sing, Adsorption by powders and porous solids: principles, methodology and applications, Academic press2013.
[12] S. Han, K. Liu, L. Hu, F. Teng, P. Yu, Y. Zhu, Superior adsorption and regenerable dye adsorbent based on flower-like molybdenum disulfide nanostructure, Scientific Reports 7 (2017) 43599.
[13] X.-Q. Qiao, F.-C. Hu, F.-Y. Tian, D.-F. Hou, D.-S. Li, Equilibrium and kinetic studies on MB adsorption by ultrathin 2D MoS_2 nanosheets, Rsc Advances 6 (2016) 11631-11636.
[14] L. Luo, M. Shi, S. Zhao, W. Tan, X. Lin, H. Wang, F. Jiang, Hydrothermal synthesis of MoS_2 with controllable morphologies and its adsorption properties for bisphenol A, Journal of Saudi Chemical Society 23 (2019) 762-773.
[15] H. Song, S. You, X. Jia, Synthesis of fungus-like MoS_2 nanosheets with ultrafast adsorption capacities toward organic dyes, Applied Physics A 121 (2015) 541-548.
[16] Z. Wan, D. Li, Y. Jiao, X. Ouyang, L. Chang, X. Wang, Bifunctional MoS2 coated melamine-formaldehyde sponges for efficient oil–water separation and water-soluble dye removal, Applied Materials Today 9 (2017) 551-559.
[17] J. Chen, Y. Liao, X. Wan, S. Tie, B. Zhang, S. Lan, X. Gao, A high performance MoO_3@MoS_2 porous nanorods for adsorption and photodegradation of dye, Journal of Solid State Chemistry 291 (2020) 121652.
[18] A.T. Massey, R. Gusain, S. Kumari, O.P. Khatri, Hierarchical microspheres of MoS_2 nanosheets: efficient and regenerative adsorbent for removal of water-soluble dyes, Industrial & Engineering Chemistry Research 55 (2016) 7124-7131.
[19] J. Wen, X. Li, W. Liu, Y. Fang, J. Xie, Y. Xu, Photocatalysis fundamentals and surface modification of TiO_2 nanomaterials, Chinese Journal of Catalysis 36 (2015) 2049-2070.